Minimax Theory and its Applications

Volume 11 (2026), No. 2s, 409 to 423

Hybrid Fuzzy-Seeker Optimization Algorithm for Dynamic Performance Enhancement of Microgrids Integrating Renewable and Storage Technologies

G. Bharathi[1], P. Kantarao[2], R. Srinivasarao[3]

[1]Research scholar, Department of EEE, JNTUK, Kakinada, AP, Indiaand Department of EEE, Shri Vishnu Engineering College for Women, Bhimavaram, AP, India. Email: bharathieee_10@svecw.edu.in, Orcid id: 0000-0003-0506-6618

[2]Department of EEE, SRKR Engineering College, Bhimavaram, AP, India. Email: dr.pkantarao@gmail.com, Orcid id: 0000-0003-2857-755X

[3]Department of EEE, JNTUK, Kakinada, AP, India. Email: srinivas.jntueee@gmail.com, Orcid id: 0000-0001-5590-4873

Abstract

This work develops a new hybrid control method for proportional power sharing among the converters of an isolated microgrid system. Several renewable energy sources, namely a photovoltaic (PV) system, a fuel cell (FC), an ultra-capacitor (UC), and a battery energy storage system (BESS), are incorporated to examine the performance of the microgrid system. A persistent challenge in PV systems, however, is extracting the maximum available power under varying weather conditions. In addition, an effective and robust control strategy is required to regulate the energy storage devices. To address these challenges, this work hybridizes fuzzy logic with the seeker optimization algorithm (SOA) to form the proposed FSOA method. A proportional-integral-derivative (PID) controller is then designed and optimized using FSOA to improve the system's dynamic stability under diverse disturbances. To demonstrate robust control under nonlinear loading and fault conditions, the dynamic response and stability of the system under the proposed method are evaluated and compared against conventional PID, fuzzy, and SOA-PID controllers. The proposed microgrid system is further tested under various loading conditions, including a 50% increment in the AC and DC loads and a 50% decrement in the DC load. The simulation results show that the proposed hybrid FSOA-PID method achieves superior dynamic response, reduced settling time, and improved accuracy compared with the other methods studied.

Keywords Renewable Energy Sources, Microgrid, Fuel cell, Ultra-capacitor, FSOA

I. Introduction

In recent years, one of the greatest global challenges has been environmental pollution and energy scarcity, caused by the rapid consumption of conventional fossil fuels and the burning of waste materials [1]. These substances release greenhouse gases such as water vapor, carbon dioxide, methane, nitrous oxide, and ozone [2]. These gases have a serious impact on weather patterns, water resources, and people's livelihoods [3]. Hence, several countries are implementing renewable, sustainable, and green energy sources to protect the environment and meet growing energy demand [4].

Owing to geographical constraints in remote areas, the utility grid cannot always supply electric power directly to consumers. In recent decades, microgrids have attracted considerable attention for power generation through renewable, sustainable, and distributed energy sources, delivering quality power supply to end users [5]. In addition to distributed generation, the distributed power system is effective for mitigating pollution, avoiding blackouts, and reducing power losses [6]. Nevertheless, several significant issues remain, such as devising an effective control strategy for optimal power sharing, an appropriate strategy for selecting micro-sources, enhancing dynamic stability under fault conditions, and active demand management.

Over the past decade, microgrid systems have incorporated renewable energy sources (RES) to enhance energy efficiency, improve system reliability, reduce energy cost, and mitigate greenhouse gas emissions [7]. However, a difficult task in renewable energy-based microgrid systems is sustaining the balance between generation and demand due to continuous climate variation [8]. Moreover, a single type of renewable energy source is not sufficient to meet load requirements [9]. The aforementioned investigations by numerous researchers

demonstrate the effects of microgrids incorporating various RES on ensuring the reliability of the power supply. Furthermore, diverse control techniques, namely DC/DC, AC/DC, and hybrid-coupled converters, are used to integrate multiple renewable sources to satisfy consumer load demand [10]. Although extensive research exists on microgrids with RES, only a few studies have focused on combining the photovoltaic (PV) system, ultra-capacitor (UC), and fuel cell [11]. Therefore, further in-depth research is necessary on this combination, together with effective control methods, to ensure reliable microgrid operation under various circumstances.

During a fault while connected to the utility grid, system inertia can deliver a high fault current to protective devices such as the inverse definite minimum time (IDMT) relay [12]. In the islanded condition, however, the microgrid system has a low-inertia state. Hence, different types of energy storage systems are required to balance power production and the desired load during fault conditions [13]. In this work, battery energy storage systems (BESS) are used to investigate their performance under various fault conditions in a renewable energy-based microgrid system [14].

Conventional controllers have been used in many studies to enhance the dynamic stability of microgrid systems. A combination of proportional-integral (PI) and proportional-derivative (PD) controllers has been presented [15]. However, these controllers may not yield productive outcomes under fault conditions, varying line parameters, or unpredictable loads, owing to their constant gain values [16]. Therefore, optimization techniques are required to obtain optimal gain values for steady-state operation of the microgrid system. Several researchers have utilized different optimization-based controllers.

There is also limited research on hybrid control methods. Given this gap in the extant literature, further research is needed to examine hybrid microgrid sources using hybrid control approaches. To the best of our knowledge, no prior study has investigated the hybridization of fuzzy logic and the seeker optimization algorithm (fuzzy-SOA) to improve microgrid system performance. The proposed system extends the microgrid configuration to include four complementary energy sources, namely PV, FC, BESS, and UC, providing the most comprehensive and robust energy management capability among the configurations examined in this study. The FSOA-PID controller is evaluated under two principal loading scenarios (50% load increment and 50% load decrement) and rigorously compared against conventional PID, standalone fuzzy, and SOA-PID controllers to establish the superiority of the proposed hybrid approach.

II. Modelling of the suggested system

The proposed microgrid system consists of various micro-sources, namely the PV system, FC, UC, and battery energy storage system (BESS)[17]. The proposed system is illustrated in Figure 1. The modelling of each micro-source is presented and explained in the following sections.

System Overview

The proposed isolated microgrid system is the most comprehensive configuration studied in this work. It integrates four distinct energy sources and storage devices:

- **Photovoltaic (PV) System**: Primary renewable generation source connected through a DC-DC boost converter with MP&O MPPT.
- **Fuel Cell (FC)**: Stable base load source connected through a DC-DC converter.
- **Battery Energy Storage System (BESS)**: Primary energy buffer for slow-to-medium timescale power imbalances, connected through a bidirectional DC-DC converter.
- **Ultra-Capacitor (UC)**: High-power, fast-response buffer for short-duration transient disturbances, connected through a DC-DC converter.

Both DC loads and AC loads are supplied from the common DC bus. The system operates in isolated (islanded) mode throughout. The proposed FSOA-DPID controller is applied to two subsystems: (1) the PV boost converter control loop via the MP&O MPPT interface, and (2) the BESS converter control loop for State of Charge (SOC) regulation and transient compensation. The UC handles instantaneous power surges while the BESS manages sustained imbalances under FSOA-PID governance. The overall proposed microgrid system is illustrated in Figure1.

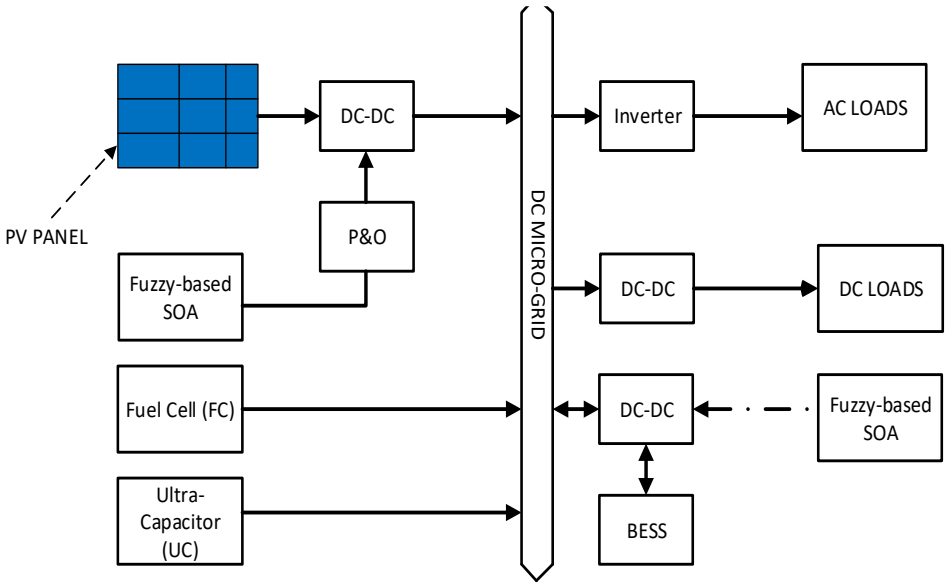


Figure 1. Proposed Microgrid system with various micro sources

A. Photovoltaic system

The electrical model of the PV system is illustrated in Figure 2. The current generated by the PV cell is represented as a non-linear DC current source (I_{ph}) resulting from solar irradiation [18]. A series resistance (R_{se}) is included to represent the sheet resistance of the semiconductor surface. In addition, the leakage current to ground when the diode is reverse-biased is represented by the shunt resistance (R_{sh})[19].

According to the Kirchhoff's current law, the current of the considered PV module is,

$$I = I_{ph} - I_d \tag{1}$$

Here, I is the PV module current, I_{ph} is the current generated by the PV cell (photocurrent), and I_d is the diode current.

The photocurrent can be expressed as,

$$I_{ph} = \left(I_{L_{ref}} + K_i \Delta T\right) \frac{G}{G_{\eta_{ref}}} \tag{2}$$

Where $I_{L_{ref}}$ indicates reference current produced by solar irradiance at steady state condition. TheK_i represents the PV cell's current temperature coefficient, and ΔT is the difference between the nominal and actual temperatures. The solar irradiance incident on the PV module surface is represented as G. Normal solar irradiance (1000 $^{W}/_{m^2}$) is reported as $G_{\eta_{ref}}$.

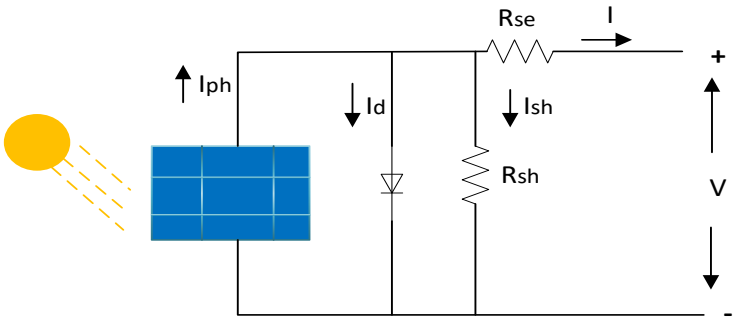


Figure 2. Demonstration of PV cell with single diode.

The diode current is expressed as[20],

$$I_d = I_o\left[e^{\left(\frac{V+R_S I}{\alpha V_t}\right)} - 1\right] \quad (3)$$

Here, I_o denotes the saturation current in the absence of solar irradiance. V_t is the PV cell thermal voltage, represented as

$$V_t = \frac{N_S K T}{q} \quad (4)$$

Here, the number of PV cells connected in series is denoted as N_S, K= Boltzmann constant (1.3806 X 10^-23 J/K), electron charge is q (1.602 X 10^-19 C), T= 25 ^{0}C (steady state condition) and α =diode ideality constant and the range is $1 < \alpha < 1.5$.

The saturation current is illustrated as,

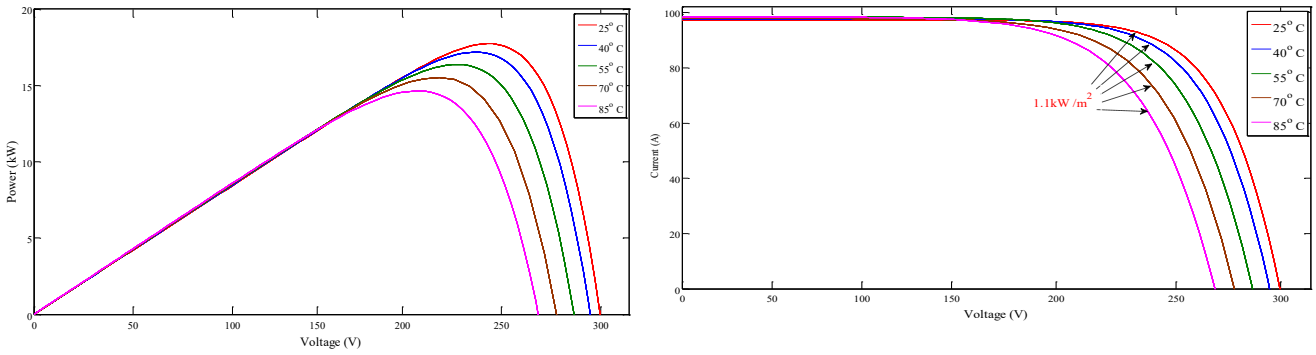
$$I_0 = I_{0,STC}\left(\frac{T}{T_{STC}}\right)^3 \exp\left(\frac{qE_G}{n.K}\right)\left(\frac{1}{T} - \frac{1}{T_{STC}}\right) \quad (5)$$

E_G denotes the semiconductor band-gap energy in eV (1.12 eV for Si).

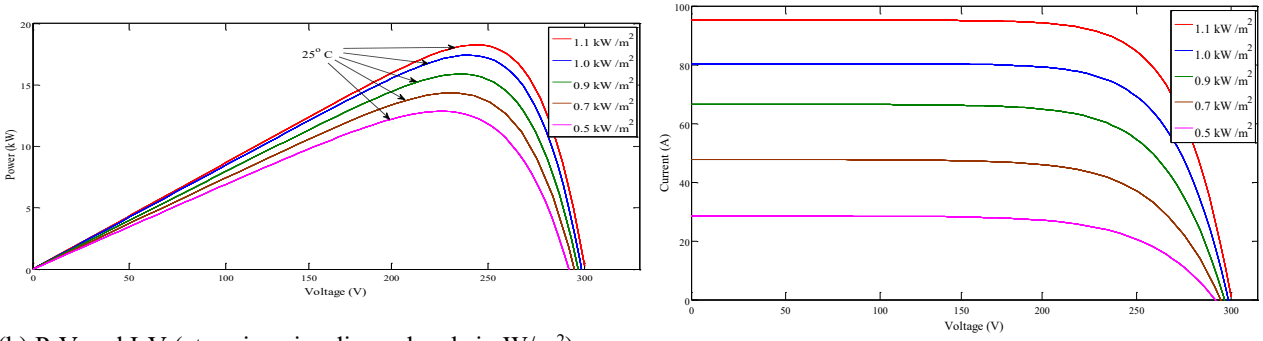
The standard saturation current is $I_{0,STC}$, which can be calculated as

$$I_{0,STC} = \frac{I_{sc,STC}}{\exp\left(\frac{V_{oc,STC}}{b.V_{t,STC}} - 1\right)} \quad (6)$$

Where $V_{t,STC}$ is the PV panel terminal voltage at standard temperature, and b is the diode constant (typically,$1 \leq b \leq 1.5$). The maximum power produced by a single PV cell is quite small (1-1.52 W). The characteristics of the PV system are demonstrated in Figure 3.



(a) P-V and I-V (at various temperatures °C)



(b) P-V and I-V (at various irradiance levels in W/m^2)

Figure 3. Characteristics of the PV at different atmospheric conditions

B. Modelling of the FC

The FC is an important device integrated into the microgrid system to enhance steady-state stability under nonlinearities[21]. When the PV system is incorporated into the microgrid, the FC can be effectively employed to compensate for fluctuations and deliver a reliable power supply. The FC is modelled as

$$G_{FC}(s) = \frac{K_{FC}}{1 + S.T_{FC}} \tag{7}$$

C. Modelling of the UC

The UC is a prominent device in electrical power systems for enhancing transient and dynamic stability under nonlinearities. In this study, the UC operates in combination with the FC and BESS to sustain power generation and meet the required load without interruption. The UC is modelled as[22],

$$G_{UC}(s) = \frac{K_{FC}}{1 + S.T_{FC}} \tag{8}$$

D. Modelling of the BESS

The BESS is an effective device for sustaining steady-state and dynamic stability under various uncertainties[23]. Since the integration of the PV system and its intermittent nature affects system performance, the BESS can be employed as a key device to improve system performance during charging and discharging. The BESS is modelled as

$$G_{BESS}(s) = \frac{K_{BESS}}{1 + S.T_{BESS}} \tag{9}$$

Table 1. Key Simulation Parameters of PV / FC / BESS / UC Microgrid

Component	**Parameter**	**Value**
PV System	Rated Power	11 kW
PV System	Nominal Voltage	440 V
PV System	Boost Output	880 V
Fuel Cell	Rated Power	65 kW, K_{FC} = 1.0, T_{FC} = 4.0 s
BESS	Rated Capacity	2500 Ah, 880 V
UC	Gain K_{UC}	1.0
UC	Time Constant T_{UC}	0.9 s
DC Bus	Nominal Voltage	880 V
DC Load (nominal)	Power	60 kW
AC Load (nominal)	Power	19 kW

III. Control approach for Microgrid

In this work, a new fuzzy-based seeker-optimized DPID (FSOA-DPID) controller is applied to control the proposed system, targeting two sources: the PV system and the BESS[24]. In the PV system, the FSOA-DPID method is applied to the DC-DC boost converter to track the maximum peak power (MPP) and dynamically balance the system. At the same time, the proposed controller directs the BESS to regulate its state of charge (SOC) and manage transients during fault conditions.

A. Control of micro sources

Conventional Perturb and Observe (P&O) method

This modified P&O method is widely used in PV systems to track the maximum power; moreover, it requires fewer input parameters and can be implemented easily at low cost[25]. It offers scope for improving the parameters to enhance the output and mainly depends on the relationship between output power and its corresponding voltage. In this method, the maximum peak power (MPP) is reached when the change in output power (ΔP) with respect to the change in voltage (ΔV) equals zero (i.e., $\Delta P/\Delta V = 0$).

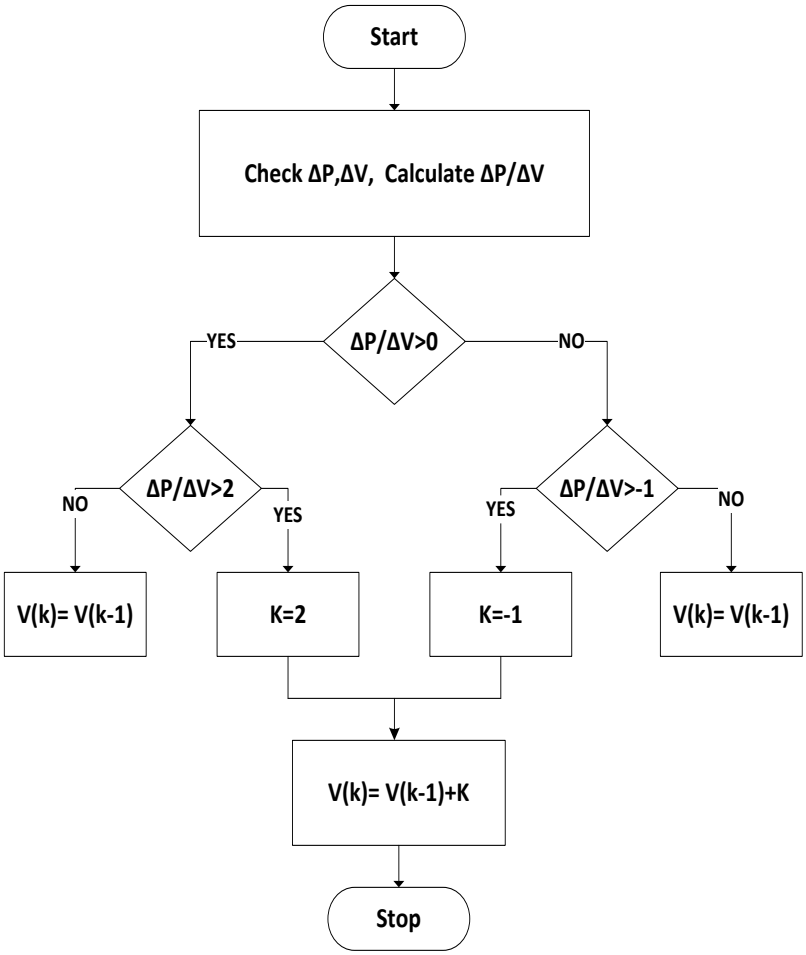


Figure 4. Flow chart for MP&O

The complete operation can be readily understood from the flow chart shown in Figure 4. As illustrated in Figure 4, a small change in voltage causes greater perturbation in power on the right side of the MPP than on the left, which is why a fixed step size K must be initialized; this is the main disadvantage of the method. In the modified P&O, an additional advantage is that an extra PV power computation is performed at the midpoint of the MPPT method.

B. Fuzzy-based seeker optimized DPID controlled MP&O method

The initialized step size (K) problem can be compensated through the proposed fuzzy-based seeker optimized DPID controlled MP&O method as shown in Figure 5.

Seeker optimization algorithm

The SOA is a new metaheuristic method and it has good searching abilities with fast convergence[26]. Moreover, this method is used in many applications, especially in power systems, to maintain the dynamic stability of the system. The SOA is based on simulating human search behavior. In this method, the entire population, consisting of numerous entities called seekers, is categorized into three subpopulations (SP)[27]. For each seeker, the neighborhood shares information based on the natural search process. The main goal of this approach is to minimize the optimization problem.

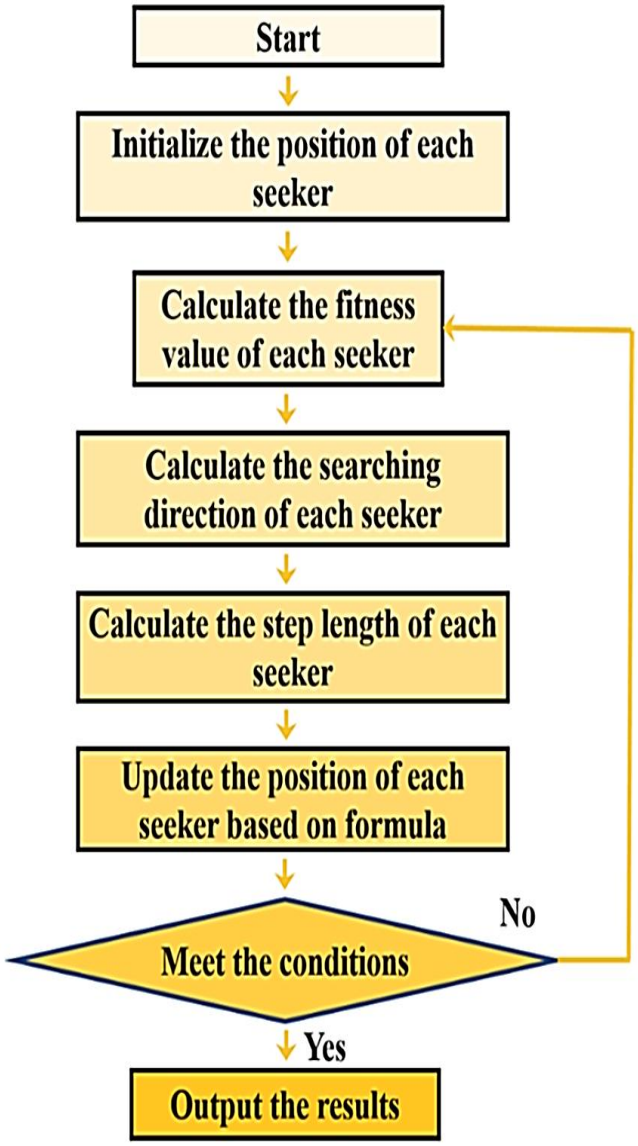


Figure 5. Flowchart of the Seeker Optimization Algorithm (SOA)

The seeker has the following characteristics: the current position $x_i = (x_{i1}, x_{i2,\ldots} x_{iD})$, its dimension 'DIM', and iteration 't'. The best position visited by the seeker itself is called p_{best}while the best position among its neighbors is called g_{best}. The search direction and step length 'SL' (SP, p, q, t) > 0 are used to update the position; these two parameters play a key role in the search process. During the search, egoistic behavior is employed, and the associated uncertainty is captured through the step length, for which a Gaussian probability distribution is used to obtain the best solutions. The updated seeker position (P) in a new dimension is represented by Equation 10.

$$\mathrm{P}(\mathrm{SP}, \mathrm{p}, \mathrm{q}, \mathrm{t}+1) = \mathrm{P}(\mathrm{SP}, \mathrm{p}, \mathrm{q}, \mathrm{t}) + \mathrm{SL}(\mathrm{SP}, \mathrm{p}, \mathrm{q}, \mathrm{t}) * \mathrm{DIM}(\mathrm{SP}, \mathrm{p}, \mathrm{q}, \mathrm{t}) \tag{10}$$

The crossover operation is used to merge the worst seeker position with the best seeker position within a subpopulation. This avoids premature convergence, and information exchange within the SP is also carried out, as shown in Equation 11.

$$\begin{cases} P(SP, m, q, t)_{\text{worst}} = \mathrm{P}(\mathrm{a}, \mathrm{q}, \mathrm{t})_{\text{best}} & \text{if } \leqslant 0.5 \\ P(SP, m, q, t)_{\text{worst}} & \text{else} \end{cases} \tag{11}$$

Here the q^{th} dimensions of m^{th} worst and the best seeker are $\mathrm{P}(\mathrm{SP}, \mathrm{m}, \mathrm{q}, \mathrm{t})_{\text{worst}}$, $\mathrm{P}(\mathrm{a}, \mathrm{q}, \mathrm{t})_{\text{best}}$.

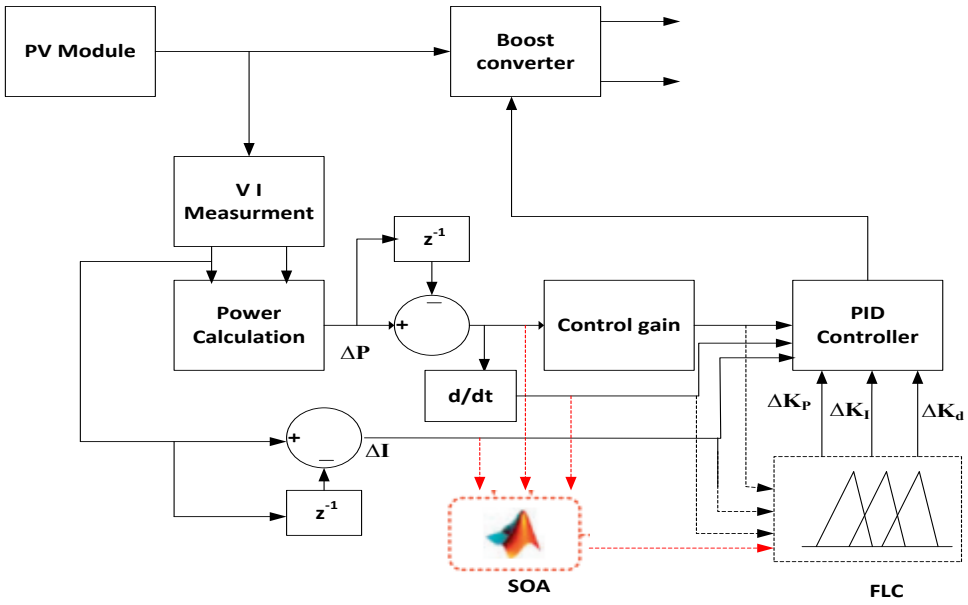


Figure 6. Fuzzy based seeker optimized DPID controller with MP&O Method

Tuning of PID parameters through FSOA

The seeker optimization algorithm reduces the integral absolute error (IAE), while the derivative term predicts the change in error [24]. Here ΔP and ΔI are the input parameters for the fuzzy logic controller (FLC) as shown through Equation 12.

$$\Delta P = P(K) - P(K-1); \Delta I = I(K) - I(K-1) \quad (12)$$

Then the fuzzy logic controller output can be represented as

$$\Delta K_P = K_P(k) - K_P(k-1) \quad (13)$$

$$\Delta K_i = K_i(k) - K_i(k-1) \quad (14)$$

$$\Delta K_d = K_d(k) - K_d(k-1) \quad (15)$$

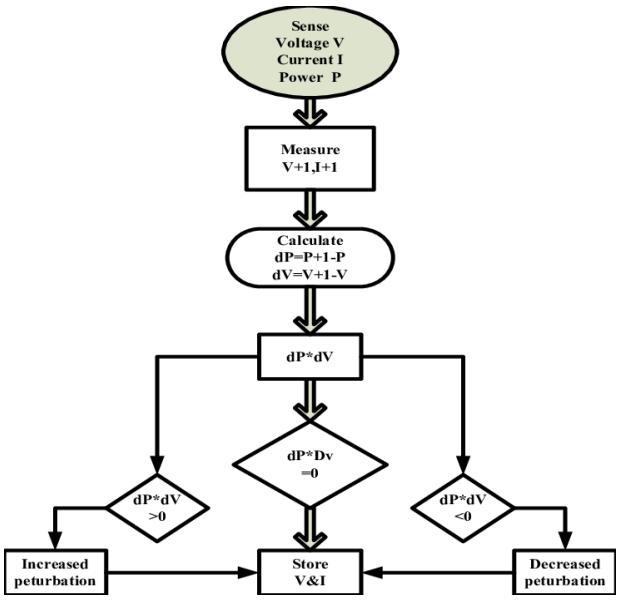


Figure 7. Complete control flow of the FSOA-DPID with MP&O

IV. Results and Discussions

In this work, a microgrid system combining PV, FC, UC, BESS, and loads is considered to investigate system performance under sudden DC load increment, DC load decrement, and AC load increment. Further, a hybrid combination of fuzzy- and SOA-based PID control is implemented to enhance the dynamic performance of the system under these distinct conditions. The analysis of the proposed system under various circumstances is presented below.

Case- A: 50 % Increment in DC and AC loads

In this scenario, the DC load on the PV/BESS/UC/FC-based microgrid system is suddenly increased by 50%. Due to the sudden changes in the DC and AC loads, the system is affected and finds it difficult to match generation with the power supplied to the users. However, the BESS unit included in the proposed microgrid system helps overcome these power difficulties. When the load increases suddenly, the battery bank promptly switches to discharging mode to stabilize power generation and meet the load requirement; it subsequently returns to its normal state once the DC/AC loads are stabilized. Battery banks are thus an effective storage device for protecting the power system against uncertain conditions. In this work, the hybrid FSOA-based PID method is proposed to minimize the changes in boost converter power, fuel cell output power, battery output power, ultra-capacitor output power, and DC bus voltage. The effectiveness of the proposed hybrid FSOA-PID is further compared with other methods, namely PID, fuzzy, and SOA-PID. Figures (6-10) present the output powers of the boost converter, fuel cell, battery, ultra-capacitor, and DC bus voltage for the various control methods. The simulation findings show that the proposed FSOA-PID method achieves greater performance in terms of settling time, overshoot, and power quality improvement compared with the other methods studied.

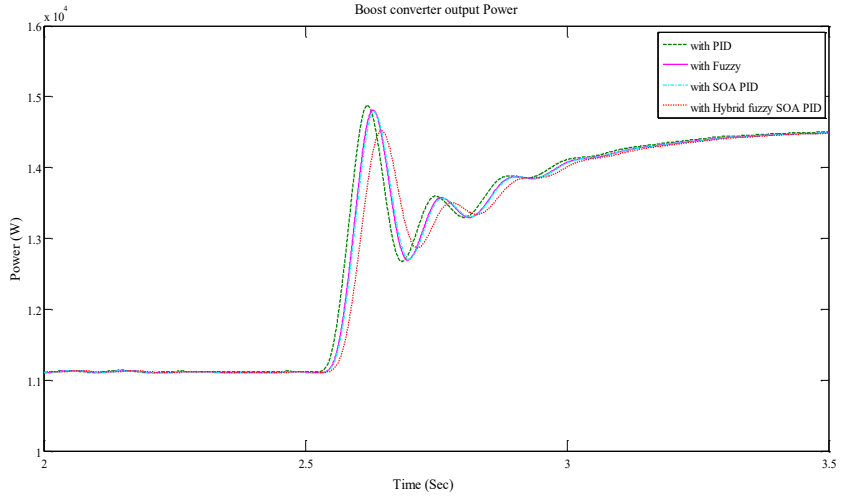


Figure 8. Boost converter output power

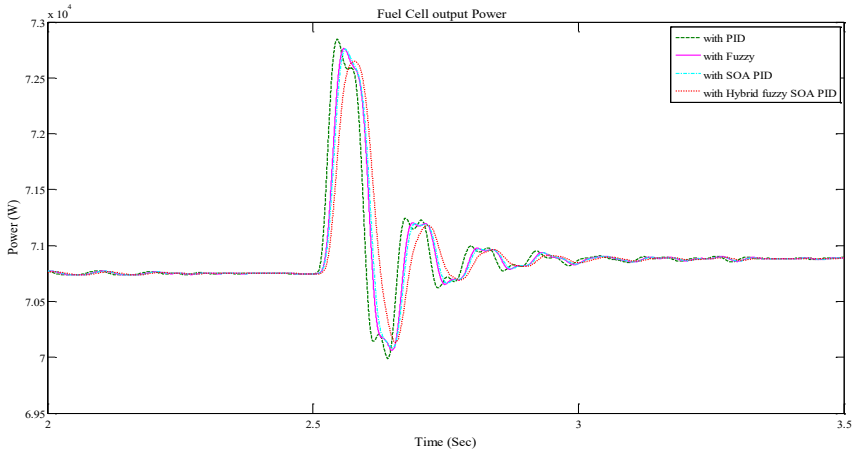


Figure 9. Fuel cell output power

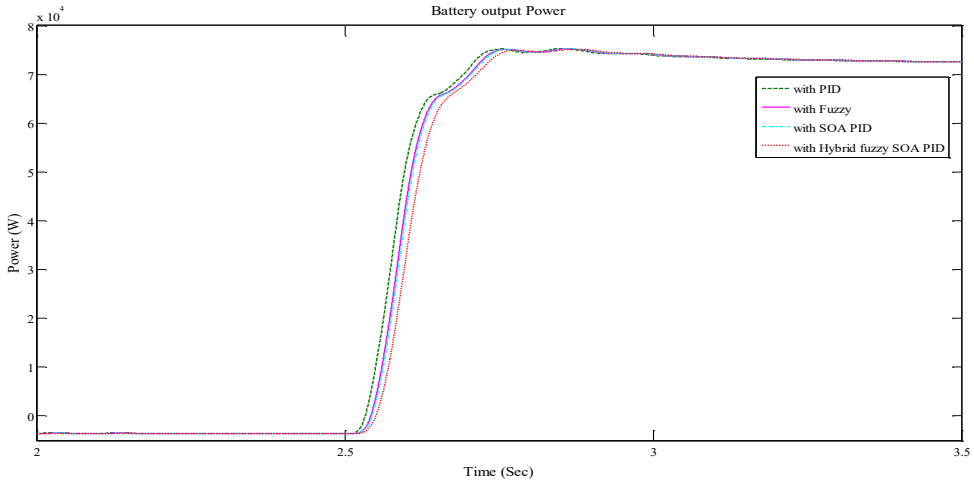


Figure 10. Battery output power

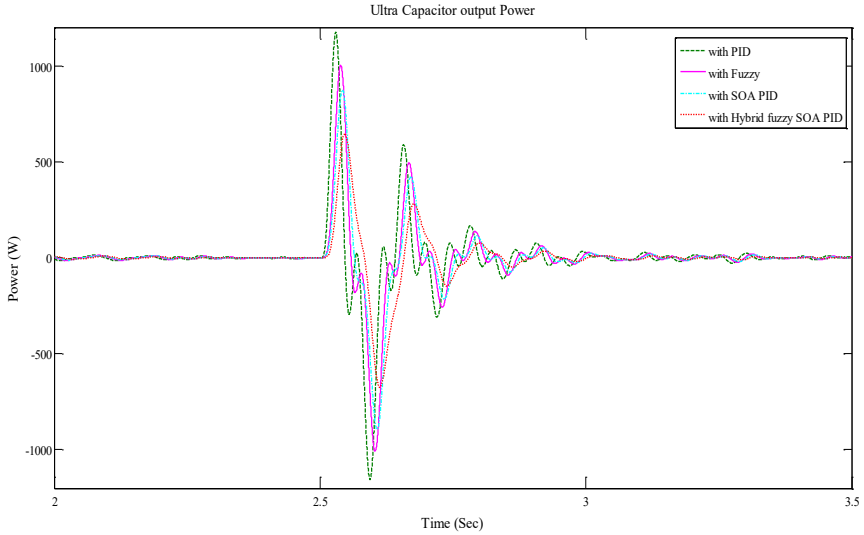


Figure 11. Ultra-capacitor output power

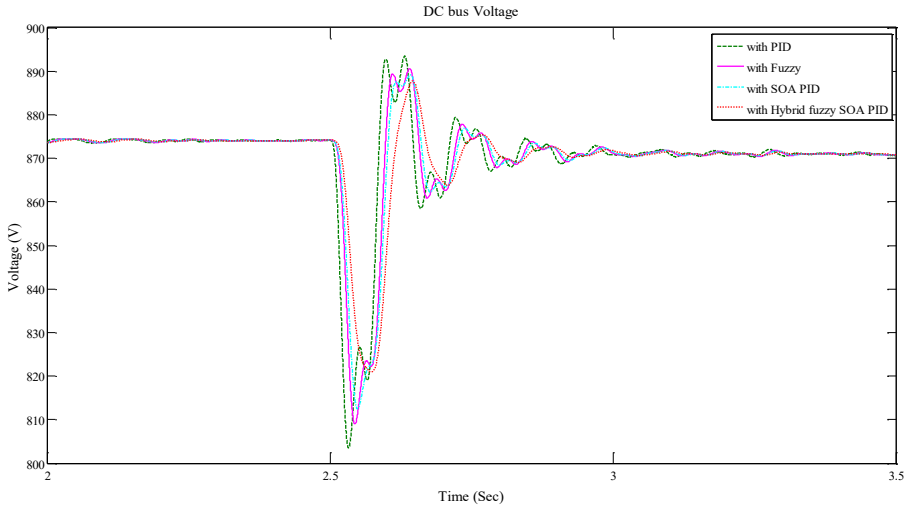


Figure 12. DC bus voltage

Table 2. Performance Comparison Under 50% DC and AC Load Increment (Scenario 1)

Output	Performance Metric	PID	Fuzzy	SOA-PID	FSOA-PID	Improvement vs PID
Boost Converter	Overshoot (W)	1.49×10^4	1.48×10^4	1.47×10^4	1.35×10^4	9.4% reduction
Boost Converter	Settling Time (s)	2.4	2.32	2.2	2.0	16.7% reduction
Fuel Cell	Overshoot (W)	7.14×10^4	7.14×10^4	7.135×10^4	7.1×10^4	0.6% reduction
Fuel Cell	Settling Time (s)	2.4	2.32	2.28	2.1	12.5% reduction
Battery	Overshoot (W)	7700	7300	6800	4200	45.5% reduction
Battery	Settling Time (s)	2.48	2.42	2.32	2.1	15.3% reduction
Ultra-Capacitor	Overshoot (W)	400	380	360	270	32.5% reduction
Ultra-Capacitor	Settling Time (s)	3.4	3.3	3.25	3.2	5.9% reduction
DC Bus Voltage	Overshoot (V)	900	896	890	880	100% elimination
DC Bus Voltage	Settling Time (s)	3.2	3.0	2.9	2.7	15.6% reduction

Case-B: 50 % Decrement in DC load

In this case, the DC load on the proposed microgrid system, combining PV/BESS/FC/UC, is suddenly decreased to 50% of the total load. The battery banks of the proposed system switch to charging mode/normal state as the DC load decreases. If the load increases rapidly, the charged battery banks switch to discharging mode to stabilize the fluctuations in the system. In this work, different control methods, namely PID/Fuzzy/SOA-PID/FSOA-PID, are used to examine microgrid performance under a sudden decrement in DC load. Moreover, the output power of the boost converter, fuel cell, battery bank, ultra-capacitor, and DC bus voltage is demonstrated in Figures (11-15). Based on the simulation outcomes, the hybrid FSOA-based PID controller outperformed the other existing methods in improving the dynamic performance of the system.

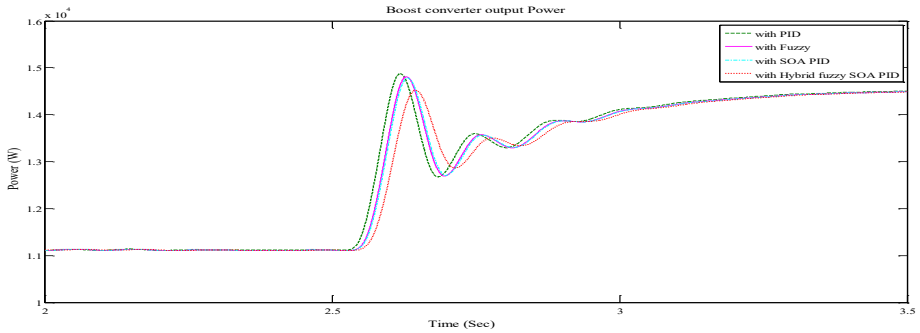


Figure 13. Boost Converter output at DC load decrement

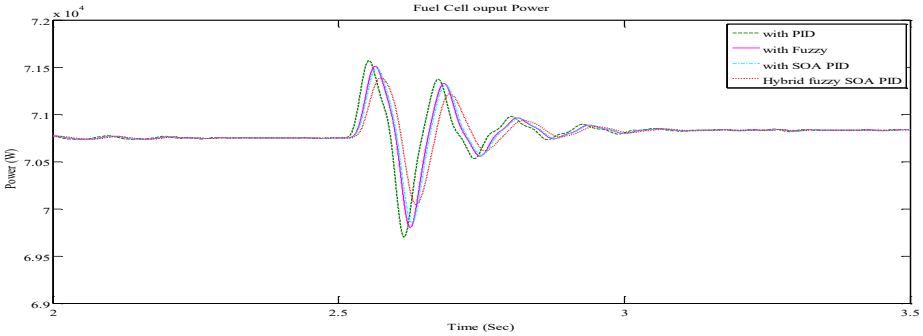


Figure 14. Fuel cell output at DC load decrement

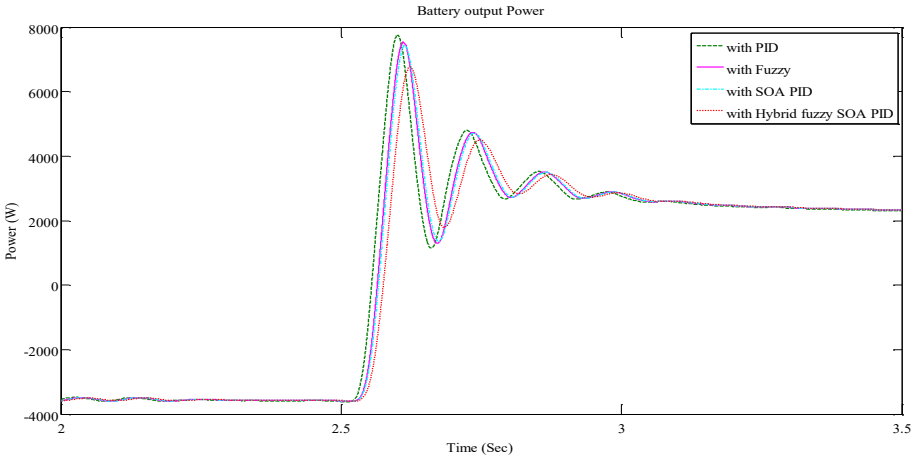


Figure 15. Battery output at DC load decrement

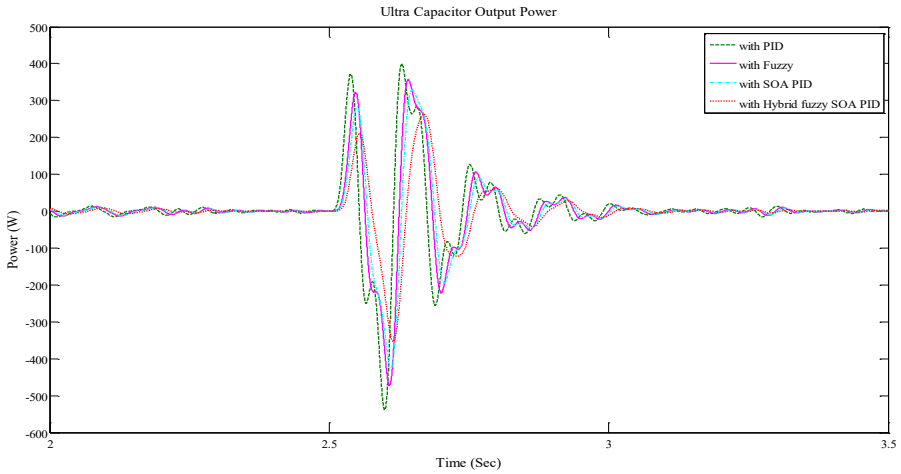


Figure 16. Ultra-capacitor output at DC load decrement

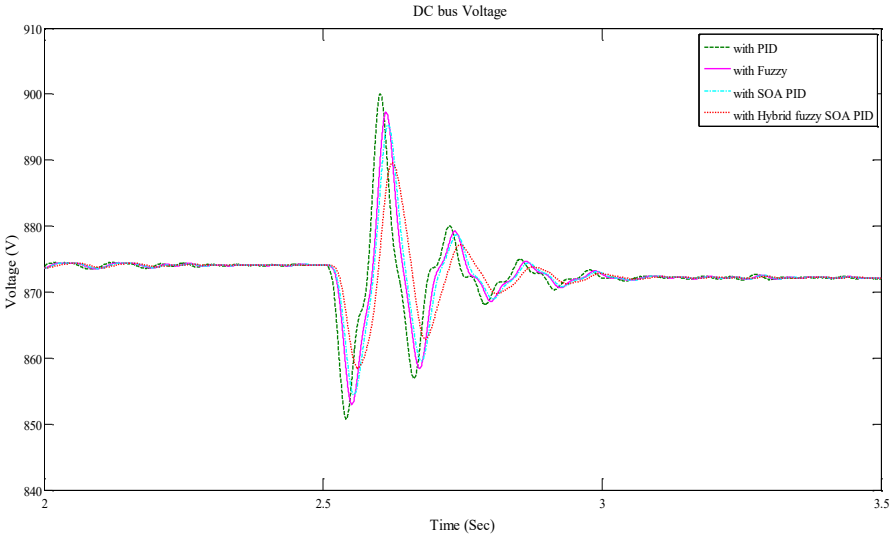


Figure 17. DC bus voltage output at DC load decrement

Table 3. Performance Comparison Under 50% DC Load Decrement (Scenario 2)

Output	Performance Metric	PID	Fuzzy	SOA-PID	FSOA-PID	Improvement vs PID
Boost Converter	Undershoot (W)	1.85×10^4	1.85×10^4	1.81×10^4	1.32×10^4	28.7% reduction
Boost Converter	Settling Time (s)	3.5	3.4	3.3	3.1	11.4% reduction
Fuel Cell	Overshoot (W)	7.282×10^4	7.27×10^4	7.26×10^4	7.1×10^4	2.5% reduction
Fuel Cell	Settling Time (s)	3.3	3.2	3.1	2.6	21.2% reduction
Battery	Overshoot (W)	7700	7300	6800	4200	45.5% reduction
Battery	Settling Time (s)	3.2	3.2	3.2	3.0	6.3% reduction
Ultra-Capacitor	Overshoot (W)	1200	1000	800	500	58.3% reduction
Ultra-Capacitor	Settling Time (s)	3.4	3.2	3.1	2.8	17.6% reduction
DC Bus Voltage	Overshoot (V)	895	890	885	880	100% elimination
DC Bus Voltage	Settling Time (s)	3.2	3.1	3.0	2.8	12.5% reduction

Table 4. Progressive Improvement in DC Bus Voltage Overshoot

Control Method	Scenario 1 Voltage Overshoot (V)	Scenario 2 Voltage Overshoot (V)	Cumulative Improvement
PID (Baseline)	900 V (+2.27%)	895 V (+1.70%)	Baseline
Fuzzy	896 V (+1.82%)	890 V (+1.14%)	Partial improvement
SOA-PID	890 V (+1.14%)	885 V (+0.57%)	Significant improvement
FSOA-PID (Proposed)	880 V (0%)	880 V (0%)	Complete elimination

This table reveals a clear progressive improvement across methods. Each step in the sequence, from PID to Fuzzy, from Fuzzy to SOA-PID, and from SOA-PID to FSOA-PID, delivers a measurable improvement in voltage overshoot performance. The proposed FSOA-PID ultimately achieves complete elimination of voltage overshoot in both scenarios, representing the ideal outcome for DC bus voltage regulation.

Table 5. Overall Performance Assessment of FSOA-PID Control Strategy

Performance Aspect	Rating	Supporting Evidence
DC Bus Voltage Overshoot	Outstanding	Zero overshoot achieved in both scenarios
DC Bus Voltage Settling Time	Excellent	2.7–3.1 s across all outputs
Battery Overshoot Reduction	Excellent	45.5% reduction vs. PID in both scenarios
UC Overshoot Reduction	Excellent	32.5–58.3% reduction vs. PID
FC Settling Time	Very Good	12.5–21.2% improvement vs. PID
MPPT Performance	Excellent	Variable step MP&O eliminates tracking oscillations
Consistency (Load ↑ vs. Load ↓)	Excellent	Symmetric performance in both disturbance directions
Superiority over PID	Outstanding	Zero voltage overshoot vs. 900/895 V for PID
Superiority over Fuzzy	Significant	Consistent improvement in all metrics
Superiority over SOA-PID	Meaningful	Fuzzy online adaptation adds significant value
Practical Deployment Readiness	High	Zero overshoot + fast settling = deployable performance

V. Conclusion

In this research, diverse renewable energy sources, namely PV, BESS, FC, and UC, are considered to investigate the microgrid system under various conditions. A new hybrid combination of fuzzy logic and the SOA method (FSOA) is developed to tune the PID controller and thereby improve microgrid system performance under nonlinearities. The proposed FSOA-PID controller, integrated with the MP&O system, is introduced for the PV subsystem to track the maximum power point and thereby achieve the highest energy efficiency. The same FSOA-PID controller is also applied to the BESS module to design an improved complementary power conditioner that ensures the highest level of energy supply reliability for the microgrid. To verify efficiency, system response time, settling time, robustness, transient and sub-transient stability, and

reliability, the proposed FSOA-PID technique is subjected to nonlinear loading and fault conditions. Further, the proposed microgrid system is examined under various conditions, including a 50% load increment in the AC and DC loads and a 50% decrement in the DC load. The performance of the proposed system is evaluated against different control methods, namely PID, fuzzy, SOA-PID, and FSOA-PID controllers. The simulation outcomes reveal that the hybrid FSOA-PID control method achieves greater improvement in dynamic response, reduced settling time, and higher accuracy compared with the other methods.

Disclosure statement

No potential conflict of interest was reported by the author(s).

References

1. P. Kumar, R. K. Singh, J. Paul, and O. Sinha, “Analyzing challenges for sustainable supply chain of electric vehicle batteries using a hybrid approach of Delphi and Best-Worst Method,” Resour. Conserv. Recycl., vol. 175, p. 105879, 2021.

2. M. Etminan, G. Myhre, E. J. Highwood, and K. P. Shine, “Radiative forcing of carbon dioxide, methane, and nitrous oxide: A significant revision of the methane radiative forcing,” Geophys. Res. Lett., vol. 43, no. 24, pp. 12–614, 2016.

3. G. A. Manful and Y. Opoku-Ankomah, “Impacts of Climate Change on Water Resources in the Volta River Basin: Reducing Vulnerability and Enhancing Livelihoods and Sustainable Development,” Clim. Chang. Water Resour. Africa Perspect. Solut. Towar. an Imminent Water Cris., pp. 333–357, 2021.

4. B. C. Ervural, S. Zaim, O. F. Demirel, Z. Aydin, and D. Delen, “An ANP and fuzzy TOPSIS-based SWOT analysis for Turkey’s energy planning,” Renew. Sustain. Energy Rev., vol. 82, pp. 1538–1550, 2018.

5. S. Ullah, A. M. A. Haidar, P. Hoole, H. Zen, and T. Ahfock, “The current state of Distributed Renewable Generation, challenges of interconnection and opportunities for energy conversion based DC microgrids,” J. Clean. Prod., p. 122777, 2020.

6. M. F. Zia, E. Elbouchikhi, and M. Benbouzid, “Microgrids energy management systems: A critical review on methods, solutions, and prospects,” Appl. Energy, vol. 222, pp. 1033–1055, 2018.

7. S. M. Hakimi, A. Hajizadeh, M. Shafie-khah, and J. P. S. Catalão, “Demand response and flexible management to improve microgrids energy efficiency with a high share of renewable resources,” Sustain. Energy Technol. Assessments, vol. 42, p. 100848, 2020.

8. A. Latif, S. M. S. Hussain, D. C. Das, and T. S. Ustun, “State-of-the-art of controllers and soft computing techniques for regulated load frequency management of single/multi-area traditional and renewable energy based power systems,” Appl. Energy, vol. 266, p. 114858, 2020.

9. S. Dudhani, A. K. Sinha, and S. S. Inamdar, “Renewable energy sources for peak load demand management in India,” Int. J. Electr. Power Energy Syst., vol. 28, no. 6, pp. 396–400, 2006.

10. N. Zhang, D. Sutanto, and K. M. Muttaqi, “A review of topologies of three-port DC–DC converters for the integration of renewable energy and energy storage system,” Renew. Sustain. Energy Rev., vol. 56, pp. 388–401, 2016.

11. A. Chauhan and R. P. Saini, “A review on Integrated Renewable Energy System based power generation for stand-alone applications: Configurations, storage options, sizing methodologies and control,” Renew. Sustain. Energy Rev., vol. 38, pp. 99–120, 2014.

12. M. A. Kashem and G. Ledwich, “Multiple distributed generators for distribution feeder voltage support,” IEEE Trans. Energy Convers., vol. 20, no. 3, pp. 676–684, 2005.

13. F. Brahman, M. Honarmand, and S. Jadid, “Optimal electrical and thermal energy management of a residential energy hub, integrating demand response and energy storage system,” Energy Build., vol. 90, pp. 65–75, 2015.

14. L. Luo, “Optimal scheduling of a renewable based microgrid considering photovoltaic system and battery

energy storage under uncertainty," J. Energy Storage, vol. 28, p. 101306, 2020.

15. K. Peddakapu, M. R. Mohamed, M. H. Sulaiman, P. Srinivasarao, D. J. K. Kishore, and P. K. Leung, "Cuckoo optimised 2DOF controllers for stabilising the frequency changes in restructured power system with wind-hydro units," Int. J. Ambient Energy, pp. 1–15, 2021.

16. R. S. R. K. Naidu, M. Palavalasa, and S. Chatterjee, "Integration of hybrid controller for power quality improvement in photo-voltaic/wind/battery sources," J. Clean. Prod., vol. 330, p. 129914, 2022.

17. M. Ranjan and R. Shankar, "A literature survey on load frequency control considering renewable energy integration in power system: Recent trends and future prospects," J. Energy Storage, vol. 45, p. 103717, 2022.

18. D. J. K. Kishore, M. R. Mohamed, K. Sudhakar, S. K. Jewaliddin, K. Peddakapu, and P. S. Rao, "Ultra-Short-term PV Power Forecasting Based on a Support Vector Machine with Improved Dragonfly Algorithm," in 2021 Emerging Trends in Industry 4.0 (ETI 4.0), 2021, pp. 1–5.

19. Y.-J. Wang and P.-C. Hsu, "An investigation on partial shading of PV modules with different connection configurations of PV cells," Energy, vol. 36, no. 5, pp. 3069–3078, 2011.

20. F. Ghani, G. Rosengarten, M. Duke, and J. K. Carson, "The numerical calculation of single-diode solar-cell modelling parameters," Renew. Energy, vol. 72, pp. 105–112, 2014.

21. M. Juneja, S. R. Mohanty, and S. K. Nagar, "Robust optimisation-based order reduction and stability analysis of autonomous DC microgrid with consideration of non-linearity," Int. Trans. Electr. Energy Syst., vol. 30, no. 2, p. e12228, 2020.

22. A. Dzieliński, G. Sarwas, and D. Sierociuk, "Comparison and validation of integer and fractional order ultracapacitor models," Adv. Differ. Equations, vol. 2011, no. 1, pp. 1–15, 2011.

23. V. Suresh, N. Pachauri, and T. Vigneysh, "Decentralized control strategy for fuel cell/PV/BESS based microgrid using modified fractional order PI controller," Int. J. Hydrogen Energy, vol. 46, no. 5, pp. 4417–4436, 2021.

24. S. Choudhury, T. P. Dash, P. Bhowmik, and P. K. Rout, "A novel control approach based on hybrid Fuzzy Logic and Seeker Optimization for optimal energy management between micro-sources and supercapacitor in an islanded Microgrid," J. King Saud Univ. Sci., vol. 32, no. 1, pp. 27–41, 2020.

25. M. Abdel-Salam, M.-T. El-Mohandes, and M. Goda, "An improved perturb-and-observe based MPPT method for PV systems under varying irradiation levels," Sol. Energy, vol. 171, pp. 547–561, 2018.

26. B. Shaw, A. Banerjee, S. P. Ghoshal, and V. Mukherjee, "Comparative seeker and bio-inspired fuzzy logic controllers for power system stabilizers," Int. J. Electr. Power Energy Syst., vol. 33, no. 10, pp. 1728–1738, 2011.

27. A. Banerjee, V. Mukherjee, and S. P. Ghoshal, "Seeker optimization algorithm for load-tracking performance of an autonomous power system," Int. J. Electr. Power Energy Syst., vol. 43, no. 1, pp. 1162–1170, 2012.

28. Oqlah Al-Refai, & Saed J. Al Atawneh. (2026). Sharp Criteria for Starlike and Convex Univalent Functions. *Results in Nonlinear Analysis*, *9*(2), 37–46.